International Journal of Engineering Research and Reviews ISSN 2348-697X (Online)
Vol. 4, Issue 4, pp: (1-10), Month: October - December 2016, Available at: www.researchpublish.com

Effects of Various Filter Parameters on the Myocardial Perfusion with Polar Plot Image

[1]Saiful Islam, [2]Rifat Reza, [3]Md.Mahmudul Hasan, [4]Nayan Das Mishu, [5]Khondoker Murad Hossain, [6]Zahid Hasan Mahmood

Department of Electrical and Electronic Engineering, University of Dhaka, Dhaka-1000, Bangladesh

Abstract: **In Single Photon Emission Computed Tomography (SPECT), Myocardial Perfusion is visualized in Short Axis (SA), Horizontal Long Axis (HLA), and Vertical Long Axis (VLA) slices of Left Ventricle (LV). Filtered Back Projection (FBP) is used as an image reconstruction algorithm in SPECT study. The choice of appropriate filter is a trade-off between image smoothness and sharpness of reconstructed images. The purpose of this study is to evaluate the effects of several filters including Butterworth, Generalized Hanning, Shepp Logan, Parzen filters with varying filter parameters (cut-off and order). Our finding is that Butterworth filter at cut-off 0.40 Nyquist, Parzen filter at cut-off 0.80 Nyquist, Hanning filter at 0.70 Nyquist and Shepp Logan filter at 0.50 Nyquist produce better image quality. For easier and more objective assessment of Myocardial Perfusion, Polar Plot display is introduced that represents tomographic slices in a single image (2D display) where information contained in the Short Axis slices of the Left Ventricle.**

Keywords: **SPECT, Myocardial Perfusion, HLA, VLA, FBP, Polar Plot display.**

I. INTRODUCTION

Single Photon Emission Comoputed Tomography (SPECT) is a nuclear medicne technique which is used to evaluate the perfusion of blood (i.e. supply of blood) through heart muscle as well as to diagnos the Coronary Artery Diseases (CAD) and various cardiac abnormalities such as myocardial infarction and atheromatous plaques. In its most basic form, a radiotracer is introduced into the patient body by injection, swallowing or inhalation. As radionuclides decay it emits gamma ray photons that are detected by a rotating gamma camera. Multiple projections are acquired at different angles around the patient body during the rotation. Computer translates these projections into a 3D image. These images allow expert nuclear medicine physicians to diagnose the patient’s disease [1].

The radioisotopes typically used in SPECT to label tracers are iodine-123, technetium-99m, xenon-133, thallium-201, and fluorine-18. In this study, technetium-99m is used due to its short Half-Life (6 hours). This imaging technique is superior to planar imaging methods due to its tomographic mode (i.e. cross-sectional imaging) that results in better contrast resolution than planar imaging.

In Single photon emission tomography (SPECT), Myocardial Perfusion is visualized in Short Axis (SA), Horizontal Long Axis (HLA), and Vertical Long Axis (VLA) slices of Left Ventricle (LV). Accurate diagnosis depends on the quality of tomographic images [2]. Image quality can be improved by using appropriate filter. Several types of filters are used in medical imaging. But, the choice of appropriate filter is a trade-off between image smoothness and sharpness. In this study, several filters including Butterworth, Generalized Hanning, Shepp Logan, Parzen filters with varying filter parameters (cut-off and order) are used for visual assessment of image quality.

Depending on the size of the LV, more than 30 slices are needed to represent the heart muscle. The visual assessment of a group of images is quite subjective, thus introducing a relatively high inter and intraobserver variability as well as time consuming [3]. For easier and more objective assessment of myocardial perfusion, Bulls eye imaging or cardiac polar plot has been developed which consists of a single image display of the information contained in the short axis slices of the left ventricle.

II. MATERIALS AND METHOD

A. Image Reconstruction:

During image acquisition, a standard rotating gamma camera takes multiple projections at different angles over a full 360 degree or 180 degree arc. Each angular view is known as projection or projection profile that resembles activity distribution. The gamma camera detectors acquire a set of projections at equally spaced angular intervals and thus two dimensional (2D) planar projections images are obtained Typically angle between views is 3 degree, and so a total of 120 views will be acquired over a full 360 degree arc. This 2-D intensity display of a set of projection profiles, known as a sonogram. Computer reconstructs these images by Filtered Back Projection method or Iterative method. Despite of existence novel techniques of image reconstruction, this method is still the most widely used in practical experiment in nuclear medicine centre, because of its facility and speed [4-5].

B. Filtered Back Projection:

Simple back projection results in blurring of an image. As a result image contains poor resolution and contrast which is clinically unaccepted. So, before back projection filtering is required that can permit perfect reconstruction of the original activity distribution inside the patient.

To improve resolution, filtered back projection involves a Ramp filter. This high pass filter sharpens the edges of an image as well as enhances object edge information. But the application of a perfect ramp filter will amplify the high frequencies and produce a very noisy result; with noise much worse than a normal planar image [6]. This also leads to degradation of signal-to-noise ratio (SNR).

To minimize these effects on SNR and artifacts at sharp edges Ramp filter is modified with a smoothing filter. A smoothing filter is a low pass filter which is characterized mainly by two parameters: cut-off frequency and order. The cut-off frequency is expressed in cycles per pixel or as a fraction of the Nq frequency. A high cut-off frequency improves the spatial resolution at the cost of statistical noise. A low cut-off frequency increases smoothing but degrades image contrast. So the selection of cut-off frequency is important in SPECT imaging. Another parameter order controls the slope of the filter function. A higher order results in sharp fall.

Different types of smoothing filters are available in SPECT imaging commonly used are the Butterworth filter, the Hamming filter, the Hanning filter, the Shepp-Logan filter, the Metz filter, the Wiener filter etc.

The Butterworth filter is a low pass filter mostly used in nuclear medicine, characterized by two parameters: the critical frequency, which is the point at which the filter starts its roll off to zero and the order or power [7].

A Butterworth filter in spatial domain is described by the following equation:

$$B(f) = \frac{f}{1+(\frac{f}{fc})^{2n}} \qquad (1)$$

Where, f is the spatial frequency domain, fc is the critical frequency, and n is the order of the filter.

Filtration is usually applied to projection images before reconstruction, but effect of filtration is shown on reconstructed trans axial images [8].

The Hanning (or Hann) filter is a relatively simple low pass filter, which is described by one parameter, the cutoff frequency [9]. The Hanning filter is defined in the frequency domain as follows:

$$H(f) = \begin{cases} 0.50 + 0.50cos\left(\frac{\pi f}{f_c}\right) & ,0 \le |f| \le f_c \\ 0 & otherwise \end{cases} \qquad (2)$$

Where, f are the spatial frequencies of the image and f_c is the cutoff frequency. The Hanning filter is very effective in reducing image noise because it reaches zero very quickly.

The Parzen filter is another example of a low pass filter and is defined in the frequency domain as follows equation [9] where, f are the spatial frequencies of the image and f_c is the cutoff frequency.

$$P(f) = \begin{cases} |f| - 6|f|\left(\frac{|f|}{f_c}\right) \times \left(1 - \frac{|f|}{f_c}\right)^2, & \left(|f| < \frac{f_c}{2}\right) \\ 2|f|\left(1 - \frac{|f|}{f_c}\right)^3, & \left(\frac{f_c}{2} < |f| < f_c\right) \\ 0, & (|f| \ge f_c) \end{cases} \qquad (3)$$

The Parzen filter is the most smoothing filter; it not only eliminates the high frequency noise but it also degrades the image resolution [10].

The Hamming filter is simpler than Butterworth filter, having only a single parameter to describe its shape, referred to as the cut off frequency [11]. This filter is defined in frequency domain as shown in equation (4), where (fc) is cut off frequency and (f) is spatial frequency.

$$H(f) = \begin{cases} 0.54 + 0.46cos\left(\frac{\pi f}{f_c}\right) & ,0 \leq |f| \leq f_c \\ 0 & otherwise \end{cases} \quad (4)$$

The Metz filter is a function of modulation transfer function (MTF) and it is based on the measured MTF of the gamma camera system. The MTF describes how the system handles or degrades the frequencies. The Metz restoration filter is defined in the frequency domain as follows [12].

$$M(F) = MTF(f)^{-1}[1 - (1 - MTF(f)^2)^x] \quad (5)$$

Where, f is the spatial domain and x is a parameter that controls the extent to which the inverse filter is followed before the low pass filter rolls off to zero. Equation (5) is the product of the inverse.

The Wiener filter is based on the signal to noise ratio (SNR) of a specific image. The one-dimensional frequency domain form of the Wiener filter is defined as follows [13]:

$$W(f) = MTF^{-1} \times \frac{MTF^2}{\left(MTF^2 + \frac{N}{O}\right)}, \quad (6)$$

Where MTF is the modulation transfer function of the imaging system, N is the noise power spectrum, and O is the object power spectrum.

The choice depends on several parameters such as: energy of the isotopes; the numbers of counts, and activity administration the statistical noise and the background noise level, the type of the organ being imaged, the kind of information we want to obtain from the images, the collimator that is used [14].

C. Algorithm:

Modern CT uses filtered back projection algorithm for image reconstruction. The steps are as follows:

1. Acquire projection profiles at N projection angles
2. Compute 1-D Fourier Transform of each profile
3 Apply appropriate filter to the each projection profile by Mathematical operation (convolution)
4 Compute the inverse FT of each FT profile to obtain a Modified projection profile
5 Perform conventional back projection using the filtered profile.

D. Phantom Test:

A phantom is an image which can be used to test the numerical accuracy of a 2-D image reconstruction algorithm. Accuracy test is performed on MATLAB software [15].

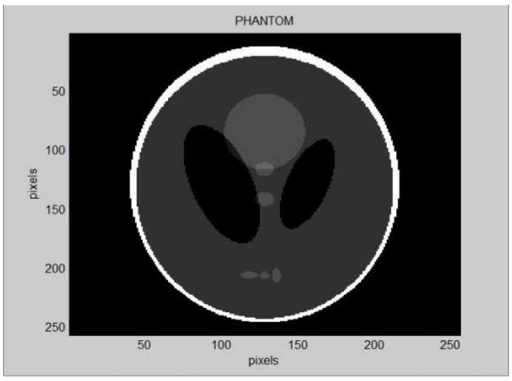

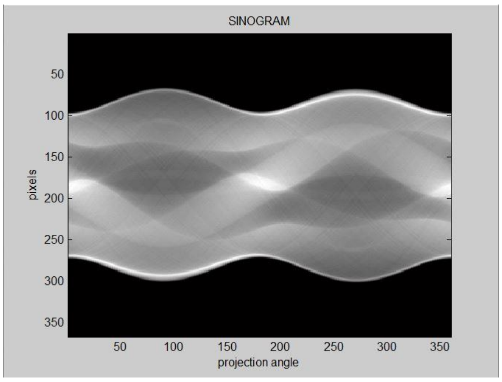

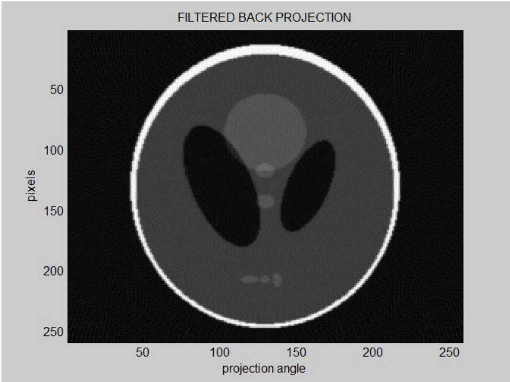

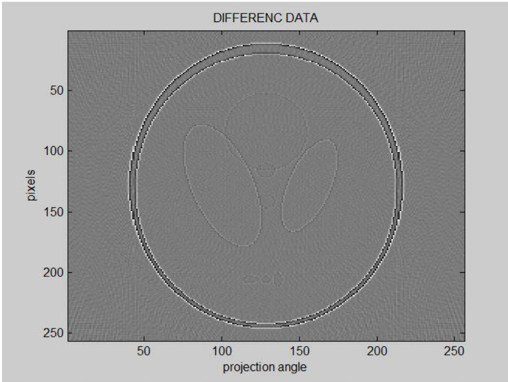

E. Imaging Protocols:

To prepare a patient for test, patient is suggested not to eat or drink anything after midnight on the night prior to test. If stomach is empty, it is less likely to become nauseous during the stress portion of the examination. The procedure begins with an intravenous injection of radionuclide contrast agent with the patient at rest. Twenty to thirty minutes later, when the radionuclide is distributed throughout the body, the patient is imaged with a gamma camera for a period of 20-30 minutes to obtain baseline cardiac images. If an exercise stress test is to be done, the patient will be taken to a treadmill and asked to exercise while their ECG is monitored.

The gamma camera used in this study was a dual head variable angle SPECT system, model SIEMENS E-CAM 12L30. This system has been equipped with low energy high resolution (LEHR) collimator and using the following acquisition parameters presented in TABLE I. For each of the protocols, the acquisition parameters are listed along with their corresponding values for exercise and rest.

TABLE I: ONE DAY STRESS-REST PROTOCOLS

Parameters	**Stress study**	**Rest study**
Radiopharmaceutical	Tc-99m (sestamibi)	Same
Dose	8-10 mCi	25-30mCi
Injection to imaging interval	20-30 min	45-60
Patient position	Supine	Same
Matrix size	64 × 64	Same
Number of views	32	Same
Mode	Step and shoot	Same
Time/projection	20 sec	Same
ECG gating	3 lead	Same
Energy peak	140 KeV	Same
Window	15%	Same

*procedure technical manual-supporting documents of National Institute of Nuclear Medicine and Allied Sciences (NINMAS), Shahbagh, Dhaka, Bangladesh.

F. Cardiac Polar Plot Display:

Polar Plot display is a 2D display of cardiac that represents a single image display of the information contained in the short axis slices of the left ventricle. In this technique short axis slices (approximately 10-14 slices) are mapped as concentric circles with the more apical slices on the inside of the display and the more basal slices on the outside. The apex is specially mapped onto the polar plot shown in Fig. 1.

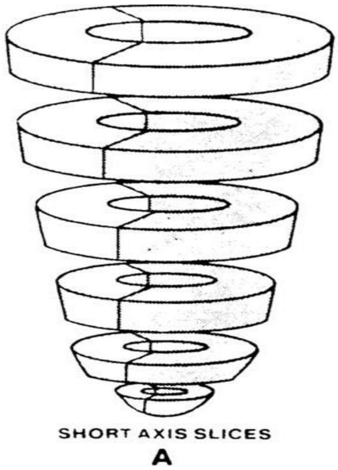

Figure 1: Mapping of short axis slices [16]

Left Ventricle (LV) is divided into 17 segments along with perfusion scoring system which is 17-segment model shown in Fig. 2.

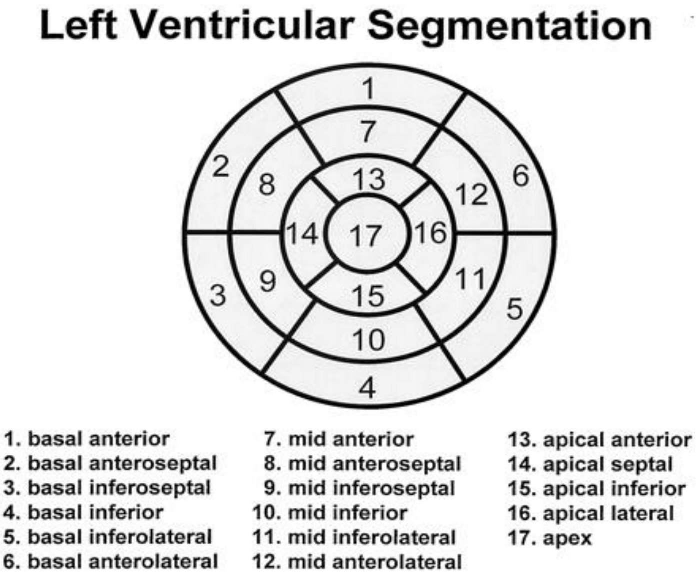

Figure 2: SPECT myocardial perfusion imaging:17-segment model [17]

Each of 17-segment of this model is analysed with a five point perfusion scoring system shown in the TABLE II.

TABLE II: A SEMIQUANTITAVIE SCORING SYSTEM

Category	**Score**
Normal perfusion	0
Mild reduction in counts—not definitely Abnormal	1
Moderate reduction in counts—definitely Abnormal	2
Severe reduction in counts	3
Absent uptake	4

In polar plot, different parametric images can be generated to show the results of quantitative analysis, "severity," and "reversibility" maps. The severity map displays the abnormal areas with the level determined by the degree of abnormality. Which is calculated as follows:

Reversibility map = summed rest score of all segments- summed stress score of all segment

International Journal of Engineering Research and Reviews ISSN 2348-697X (Online)
Vol. 4, Issue 4, pp: (1-10), Month: October - December 2016, Available at: www.researchpublish.com

III. RESULTS AND DISCUSSION

Accurate diagnosis of Coronary Artery Diseases (CAD) depends on the quality of tomographic images. The smoothing filters can greatly affect the image quality. Appropriate filter selection and adequate smoothing helps the physician in results interpretation and accurate diagnosis. The effects of several smoothing filters: Butterworth, Hanning, Shepp-Logan, and Parzen filters in Myocardial Perfusion study are shown in Fig. 3, Fig. 4, Fig. 5, Fig. 6, and Fig.7.

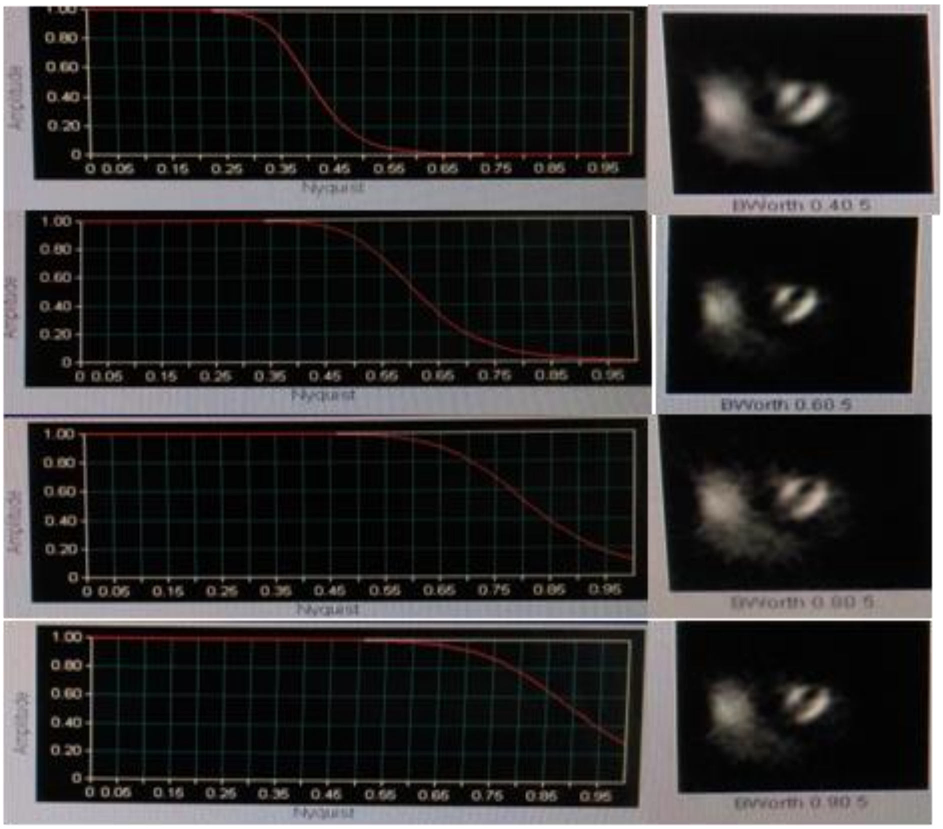

Figure 3. The effect of varying cutoff frequencies of Butterworth filter of order 5 (power factor = 10 for all critical frequencies) with FBP. First column shows myocardial slices and second column shows Butterworth curves for various cutoff frequencies (0.40, 0.60, 0.80, and 0.90) in Nyquist

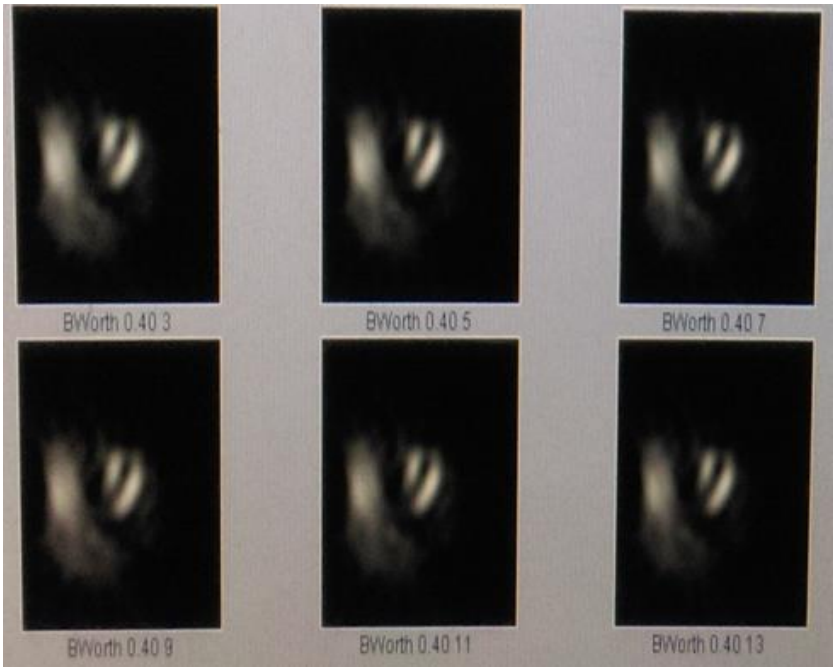

Figure 4. The effect of varying order of Butterworth filters with FBP.

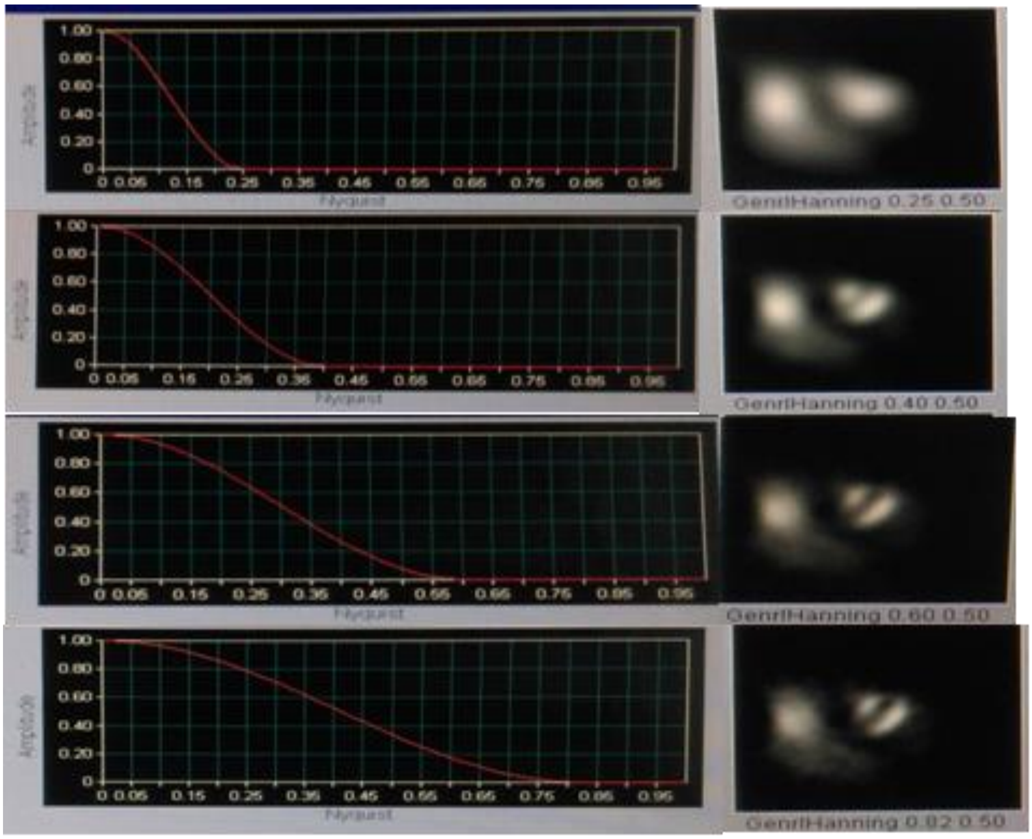

Figure 5. The effects of varying cutoff frequencies of Generalized Hanning filter with FBP. First column shows myocardial slices and second column shows Generalized Hanning curves for various cutoff frequencies (0.25, 0.40, 0.60, and 0.82) in Nyquist.

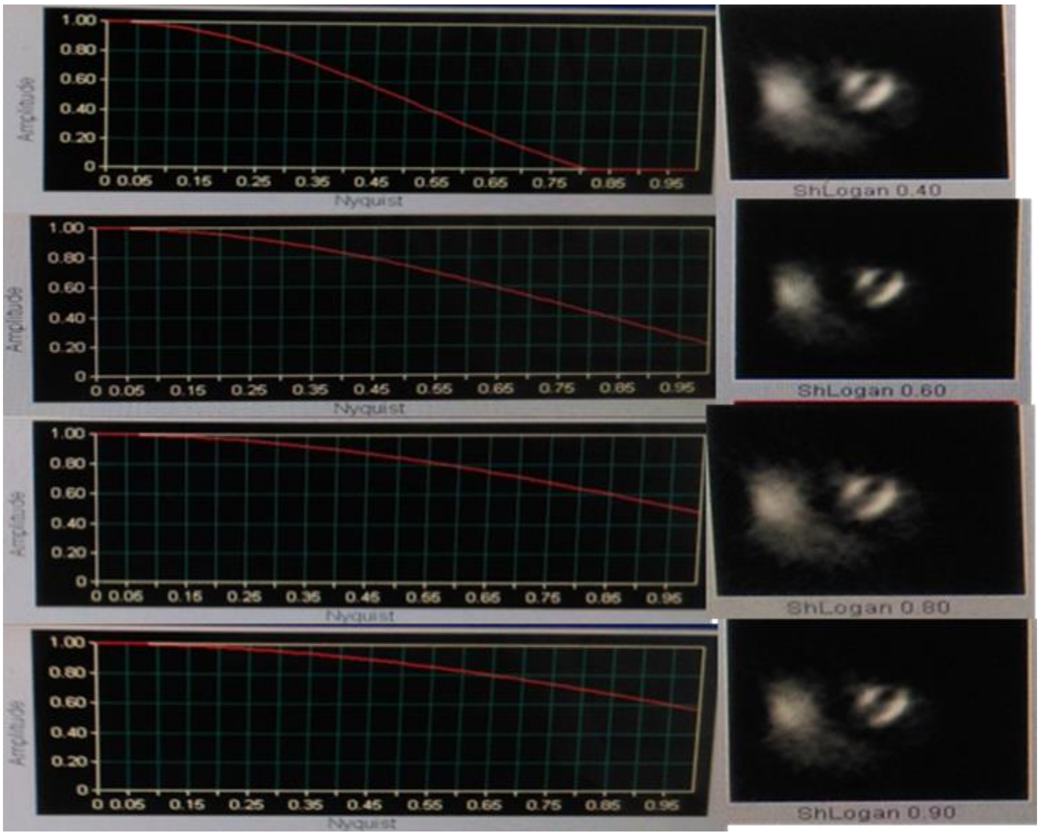

Figure 6. The effect of varying cutoff frequencies of Shepp Logan filters with FBP. First column shows myocardial slices and second column shows Sheep Logan curves for various cutoff frequencies (0.40, 0.60, 0.80, and 0.90) in Nyquist

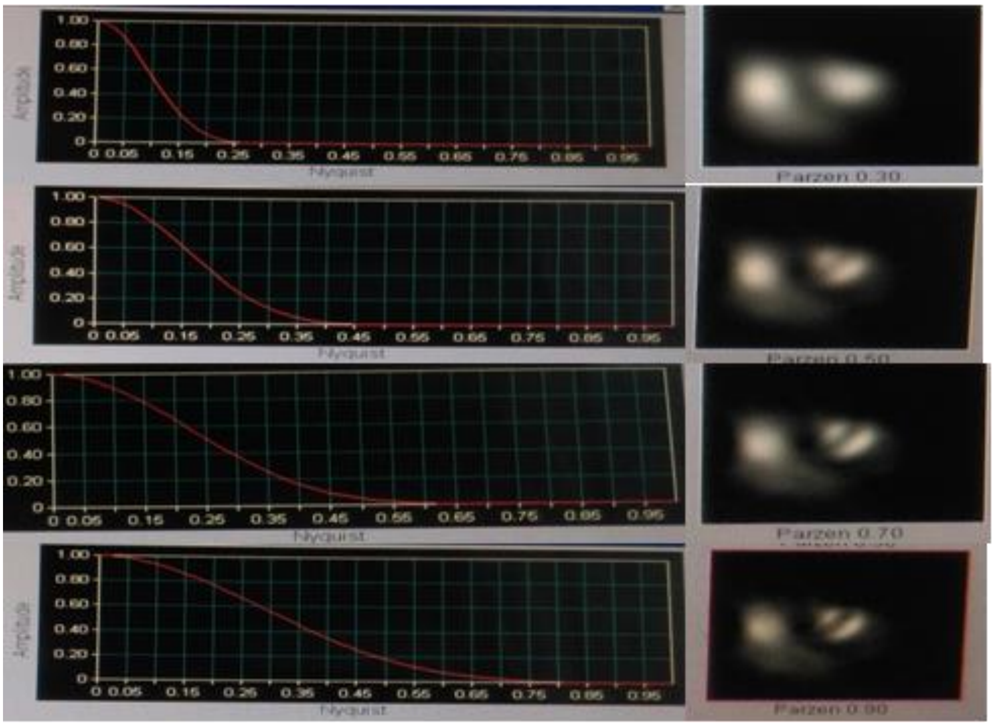

Figure 7. The effects of varying cutoff frequencies of Parzen filter with FBP. First column shows myocardial slices and second column shows Parzen curves for various cutoff frequencies (0.30, 0.50, 0.70, and 0.90) in Nyquist

The study shows that Butterworth 0.40 Nyquist, Parzen filter at cut-off 0.80 Nyquist, Hanning filter at 0.70 Nyquist and Shepp Logan filter at 0.50 Nyquist produces optimal image quality. So these cut-offs can be used as optimal for the above filters. In each of the above filters, an increase from the optimal improves the resolution but addition of noise degrades the image quality and a lower cut-off frequency from the optimal blurs the image. The study also shows that in case of Butterworth filter, a slight change in order does not affect the image quality but order 11 produces better image than order 5.

For qualitative evaluation of perfusion defects, a 17-segment semi quantitative model was analyzed during the course of this research shown in Fig. N. The severity map displays the abnormal areas with the level determined by the degree of abnormality. A reversibility map demonstrates which areas show improved perfusion at rest.

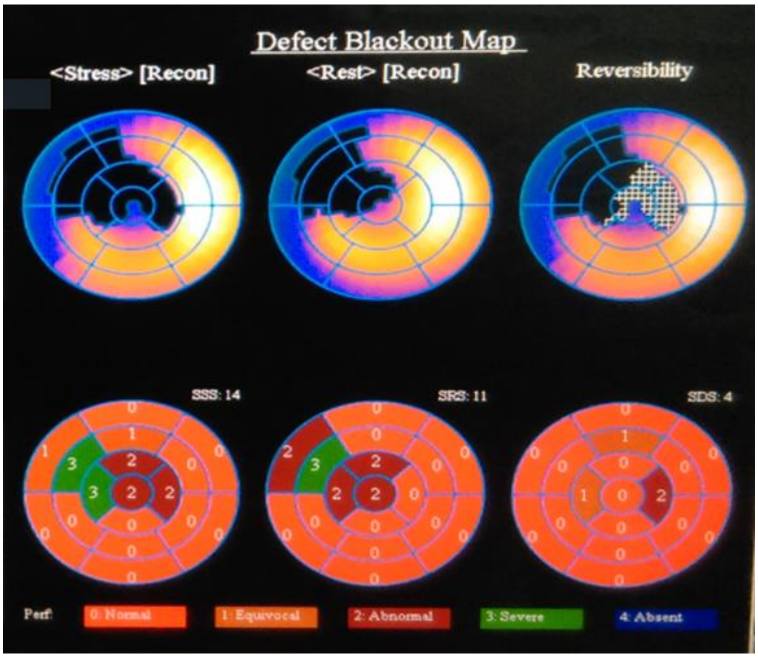

Figure N. Cardiac Polar plot display

IV. CONCLUSION

At present, SPECT Imaging test has been worldwide considered as the standard technique for the accurate diagnosis of coronary artery disease. SPECT distinctly leads to significant development than other techniques as it provides functional activity of heart both in stress and rest conditions. SPECT imaging enables the physician to acquire the 3D and 4D view of patient heart. Tc-99m with sestamibi has been used as a radiopharmaceutical in this study.

Accurate diagnosis of CAD depends on image quality. Filtered Back Projection has been used in the study as image reconstruction algorithm due to its speed, efficiency and simplicity. Proper filter selection helps the physicians in results interpretation and accurate diagnosis. Ramp filter while eliminating star artifact amplifies the statistical noise. To reduce this noise, smoothing filters like Butterworth, Shepp Logan, Generalized Hanning and Parzen are normally used in cardiac study.

This study shows that Butterworth filter at cut off 0.40 Nyquist and order 5, Parzen filter at cut-off 0.80 Nyquist, Hanning filter at 0.70 Nyquist and Shepp Logan filter at 0.60 Nyquist produce better image quality. A lower cut-off frequency from the optimal generates a thicker slice with poor edge information and a higher cut-off produces a thinner slice with higher noise. Thus, both degrade the image quality. 2D representation- Polar plot of 3D organ is used for the quantitative analysis and ease of interpretation. Severity of patient is evaluated from the difference of stress and rest plot.

Variations in the image quality may lead to false positive or false negative interpretation of the patient condition. Increasing the number of patients further work can be conducted on sensitivity and specificity of the process. With the emergence of high speed computer, 3D Iterative algorithm can be used to improve the image quality.

Further developments in cardiac diagnosis include a new promising tool, computational cardiology. Performing patient-specific computer simulations of the function of the diseased heart for either diagnostic or treatment purposes could be an exciting new implementation of computational cardiology [18].

ACKNOWLEDGMENT

We would like to express our very great appreciation to Kamila Qadir, Director, Bioscience Division, Bangladesh Atomic Energy Commission and Selim Reza, Senior Scientific Officer, Institute of Nuclear Medicine & Allied Sciences, Bangladesh Atomic Energy Commission, Dhaka Medical College for their scientific guidance during the course of this research. Also, we would like to thank chief technician Khokon Kumar, National Institute of Nuclear Medicine and Allied Science center at Bangabandhu Shiekh Mujib Medical University for their technical support in image reconstruction and patient data used in this study.

REFERENCES

[1] Simon R. Cherry, James A. Sorenson, Michael E. Phelps, "Physics in Nuclear Medicine," 4th ed, Philadelphia, PA 19103-2899, ISBN: 978-1-4160-5198-5.

[2] M. Lyra, A. Ploussi, M. Rouchota, and S. Synefia, "Filters in 2D and 3D Cardiac SPECT Image Processing," Cardiology research and practice vol.2014, 2014.

[3] G. B. Trobaugh, F. J. T. Wackers, E. B. Sokole, T. A. De Roneu, J. L. Ritchie, G. W. Hamilton, "Thallium-201 myocardial imaging: an international study of observer variability," J Nucl Med. 1978 Apr;19(4):359-363.

[4] L. A. Kunyansky, "A new SPECT reconstruction algorithm based on the Novikov explicit inversion formula," *Inverse Problems 17(2001)*, pp.293-306.

[5] T. Zeniya, H. Watabe, T. Aoi, M.Kyeong, N.Hayashi, A.Sohlberg, A. Kubo, H. Iida, "A new reconstruction strategy for image improvement in pinhole SPECT," European Journal of Nuclear Medicine and Molecular Imaging, 2004, pp.1166-1172.

[6] Patterson, Brian F. Hutton, "Nuclear assessment medicine Technologists," Understanding SPECT Part 1.Author: Brian F Hutton Module 10 Unit 19a,Regional Cooperative Agreement International Atomic Energy AgencK. van Laere, M. Koole, I. Lemahieu, and R. Dierckx, "Image filtering in single- photon emission computed tomography: Principals and applications," Computewrizzed Medical Imaging and Graphics, vol. 25, no. 2, pp.127-133, 2001.

[7] M. M. Khalil, "Basic Sciences of Nuclear Medicine," Springer, Berlin, Germany, 2010.

[8] G. Germano, "Technical aspects of myocardial SPECT imaging," Journal of Nuclear Medicine, vol. 42, no. 10, pp. 1499–1507, 2001.

[9] M. N. Salihin, A. Zakaria, "Determination of the optimum filter for qualitative and quantitative 99mTc myocardial SPECT imaging," Iranian Journal of Radiation Research, vol. 6, no. 4, pp.173–182, 2009.

[10] K. van Laere, M. Koole, I. Lemahieu, R. Dierckx, "Image filtering in single-photon emission computed tomography: Principles and applications," Computerized Medical Imaging and Graphics, vol. 25, no. 2, pp. 127–133, 2001.

[11] S. J. Cullom, " Principles of cardiac SPECT," Lippincott Williams & Wilkins, 2001, USA.

[12] M. A. King, S. J. Glick, B. C. Penney, R. B. Schwinger, P. W. Doherty, "Interactive visual optimization of SPECT prereconstruction filtering," Journal of Nuclear Medicine, vol. 28, no. 7, pp. 1192–1198, 1987.

[13] J. M. Links, R. W. Jeremy, S. M. Dyer, T. L. Frank, and L. C. Becker, "Wiener filtering improves quantification of regional myocardial perfusion with thallium-201 SPECT," Journal of Nuclear Medicine, vol. 31, no. 7, pp. 1230–1236, 1990.

[14] G. V. Heller, A. Mann, and R. C. Hendel, " Nuclear Cardiology: Technical Applications," Mcgraw-Hill, New YORK, NY,USA,2009.

[15] www.mathworks.com.

[16] Kathryn A. Morton, "The Use of Computer-Assisted Diagnosis in Cardiac Perfusion Nuclear Medicine Studies: A Review (Part 2)," Journal of Digital Irnaging, Vol 6, No 1 (February), 1993: pp 1-15.

[17] M. D. Cerqueira, N. J. Weissman, V. Dilsizian, A. K. Jacobs, S. Kaul, "Standardized myocardial segmentation and nomenclature for tomographic imaging of the heart," pp.539-542, 2002.

[18] N. Trayanova, "Computational cardiology: the heart of the matter," *ISRN Cardiology*, vol. 2012,Article ID269680, 15 pages, 2012.